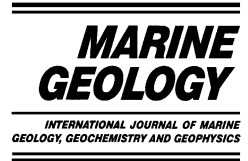




ELSEVIER

Marine Geology 195 (2003) 153–176



www.elsevier.com/locate/margeo

Seabed morphology and hydrocarbon seepage in the Gulf of Cádiz mud volcano area: Acoustic imagery, multibeam and ultra-high resolution seismic data

L. Somoza^{a,*}, V. Díaz-del-Río^b, R. León^a, M. Ivanov^c,
M.C. Fernández-Puga^a, J.M. Gardner^d, F.J. Hernández-Molina^e,
L.M. Pinheiro^f, J. Rodero^g, A. Lobato^b, A. Maestro^a, J.T. Vázquez^e,
T. Medialdea^a, L.M. Fernández-Salas^b

^a Marine Geology Division, IGME, Geological Survey of Spain, Rios Rosas 23, 28003 Madrid, Spain

^b Centro Oceanográfico de Málaga, Instituto Español de Oceanografía, Fuengirola, 29640 Malaga, Spain

^c UNESCO Center on Marine Geology and Geophysics, Moscow State University, Geology Faculty, Moscow, Russia

^d Naval Research Laboratory, Marine Geosciences Division, Code 7420, Washington, DC 20375, USA

^e Facultad de Ciencias del Mar, University of Cádiz, Puerto Real, 11510 Cadiz, Spain

^f Departament of Geosciences, University of Aveiro, 3800-193 Aveiro, Portugal

^g Instituto Andaluz de Ciencias de la Tierra, CSIC/University of Granada, 18071 Granada, Spain

Received 2 June 2001; accepted 5 November 2002

Abstract

Extensive mud volcanism, mud diapirism and carbonate chimneys related to hydrocarbon-rich fluid venting are observed throughout the Spanish–Portuguese margin of the Gulf of Cádiz. All the mud volcanoes and diapirs addressed in this paper lie in the region of olistostrome/accretionary complex units which were emplaced in the Late Miocene in response to NW-directed convergence between the African and Eurasian plates. The study area was investigated by multibeam echo-sounder, high and ultra-high resolution seismic profiling, dredging and coring. The structures observed on multibeam bathymetry, at water depths between 500 and 1300 m, are dominated by elongate mud ridges, mud cones, mud volcanoes and crater-like collapse structures ranging in relief from 50 to 300 m and size from 0.8 to 2 km in diameter. The main morphotectonic features, named the Guadalquivir Diapiric Ridge (GDR) and the Cádiz Diapiric Ridge (CDR), are longitudinally shaped diapirs which trend NE–SW and consist of lower–middle Miocene plastic marly clays. The GDR field and the TASYO field, which consist of mud volcanoes and extensive fluid venting related to diapiric ridge development, are described in this paper. The GDR field is characterised by numerous, single, sub-circular mud volcanoes and mud cones. The single mud volcanoes are cone-shaped features with relatively gentle slopes of 3°–6°, consisting of several generations of mud breccia deposition with indications of gas-saturation, degassing structures and the presence of H₂S. The mud cones have asymmetric profiles with steep slopes of up to 25° and contain large surficial deposits of hydrocarbon-derived carbonate chimneys and slabs. The TASYO field is characterised by an extensive concentration of small, sub-circular depressions, oval and multi-cone mud volcanoes and large sediment slides. Mud volcanoes in this area are characterised by moderate slopes (8°–12°),

* Corresponding author. Tel.: +34-91-8043735. E-mail address: l.somoza@igme.es (L. Somoza).

have bathymetric relief ranging from 100 to 190 m and consist of sulphide-rich mud breccia, calcite chimneys, carbonate crusts and chemosynthetic fauna (Pogonophora tube worms). We propose that all these hydrocarbon seepage structures are related to lateral compressional stress generated at the front of the olistostromic/accretionary wedge. This stress results in the uplifting and squeezing plastic marly clay deposits. Additionally, the compressional stress at the toe of the olistostrome forms overpressurised compartments which provide avenues for hydrocarbon-enriched fluids to migrate.

© 2003 Elsevier Science B.V. All rights reserved.

Keywords: mud volcanoes; carbonate mounds; diapirs; hydrocarbon seeps; chemosynthetic fauna; gas hydrates

1. Introduction

Numerous investigations world-wide (recently summarised by Milkov, 2000) have shown that hydrocarbon-enriched fluid venting produces specific structures on the sea floor (Hedberg, 1974; Hovland and Judd, 1988) in a wide variety of geologic environments, including passive continental margins dominated by salt tectonics similar to what has been observed in the Gulf of Mexico (Roberts and Carney, 1997), transform zones in Monterey Bay (Orange et al., 1999) and convergent plate boundaries found at the Mediterranean Ridge (Ivanov et al., 1996), Black Sea (Limonov et al., 1997), and Barbados Ridge (Brown and Westbrook, 1988). However, the importance of deep submarine seepage related to the olistostrome/accretionary wedge of the Gulf of Cádiz, the westernmost arc of the Alpine–Mediterranean compressional system (Fig. 1), has remained uncertain until the recent use of new technologies such as multibeam bathymetry echo-sounders and long-range sidescan sonars for deep marine exploration. Cooperation between the TASYO project and the UNESCO–IOC Training Through Research (TTR) programme have permitted us to identify numerous structures caused by hydrocarbon seepage related to tectonic compression and olistostrome development in the Gulf of Cádiz (Fig. 2).

In the Gulf of Cádiz, gas-venting has formed pockmarks along the shelf break of the Spanish margin (Baraza and Ercilla, 1996). Several mud volcano fields, attributed to the venting of fluids oversaturated in methane, and the presence of hydrates and authigenic carbonates (Ivanov et al., 2000; Somoza et al., 2000; Gardner, 2001) have also been identified. According to the results of

gas measurements, these areas are characterised by relatively high background gas content (up to 292 ml/l) in comparison to other areas of extensive mud volcanism such as the Eastern Mediterranean and the Black Sea (Stadniskaia et al., 2000). The first mud volcano discovered in the Gulf of Cádiz was identified in 1999 on Seamap 12 kHz sidescan sonar images collected by the Naval Research Laboratory (NRL) and verified by sediment sampling on the TTR-9 cruise in 1999 aboard R/V *Professor Logachev* (Gardner, 1999; Ivanov et al., 2000; Gardner, 2001). Two active (Yuma and Ginsburg) and three inactive mud volcanoes (TTR, Kidd and Adamastor) were surveyed and sampled (Fig. 2) on the continental margin of Morocco (Gardner, 1999; Gardner, 2001). The cruise TASYO-2000 aboard the R/V *Hespérides* led to the discovery of the TASYO field on the continental margin of Spain (Fig. 2), an area of extensive deep fluid flux through the sea floor on the Gulf of Cádiz slope (Somoza et al., 2000). The area was surveyed using multibeam echo-sounder and ultra-high resolution seismic profiling. A large number of mud volcanoes, numerous pockmarks, and features resembling scars of a large sediment slide migrating towards the Horseshoe abyssal plain were identified in the multibeam and seismic records. During the TTR-10 cruise aboard R/V *Professor Logachev*, several mounds, which were hypothesised to be mud volcanoes, were surveyed. These mud volcanoes occur on the lower slope of the Deep Portuguese Margin (DPM) (Fig. 2) and have been named Bonjardim, Olenin and Ribeiro mud volcanoes (Ivanov et al., 2001). On the Moroccan margin, close to the region previously surveyed during TTR-9 and TASYO-2000 cruises, mud breccia and carbonate slabs were collected from

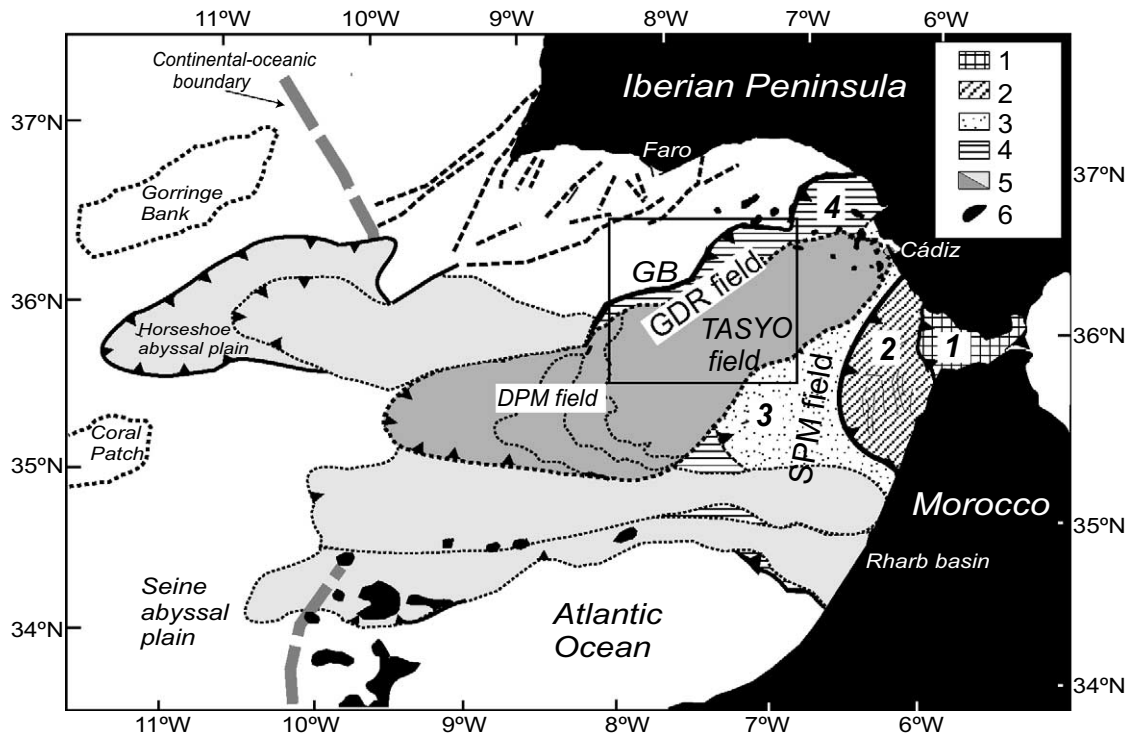


Fig. 1. Structural map of the study area showing the relationship between tectono-sedimentary units (modified from Somoza et al., 1999) and location of the mud volcano fields in the Gulf of Cádiz. Tectono-sedimentary units of the Gibraltar arc: 1 = Campo de Gibraltar Flysch complex; 2 = external units (Lower Jurassic–Palaeocene); 3 = Triassic Diapiric Zone; 4 = front of the late Tortonian deformed wedge (Early–Middle Miocene); 5 = allochthonous mass wasting and salt nappes, ‘olistostromes and precursory olistostromes’ (Late Tortonian to Present); 6 = salt diapirs. GB = Guadalquivir Bank (Palaeozoic and Mesozoic basement of the Iberian passive margin). Mud volcano fields: SM = Spanish–Moroccan field (Gardner, 1999; Ivanov et al., 2000; Gardner, 2001); DPM = Deep Portuguese margin field (Ivanov et al., 2001); GDR = Gualdalquivir Diapiric Ridge field and TASYO field (in this paper). Inset box shows the location of the study area.

mud volcanoes which have been named Rabat, Student, Baraza and TASYO (Fig. 2). During the cruise Anastasya-2000, aboard the R/V *Cornide de Saavedra*, several new mud volcanoes, which were previously identified on seismic and multibeam bathymetry data, and large fields of hydrocarbon-derived carbonate chimneys, were sampled (Díaz del Río et al., 2001).

It is important to point out that we define mud volcanoes as edifices which have been built up by the eruption of mud breccia triggered by the vertical migration of hydrocarbon-rich fluids (Guliyev and Feizullayev, 1997), in contrast to the term mud diapirs, which do not eject fluidised sediment (Milkov, 2000). In contrast, we use the term mud cone to describe an edifice produced by

the intrusion of viscous gas-charged muds (Camerlenghi et al., 1995). In the Gulf of Cádiz, we have observed that mud cones can produce structures related to hydrocarbon seepage such as carbonate chimneys without building up a mud breccia edifice.

This paper will examine fluid migration in the Gulf of Cádiz and how it relates to new venting structures observed on multibeam data, high to ultra-high resolution seismic data and verified through sampling.

2. Geological setting

The Gulf of Cádiz (Fig. 1) is located at the

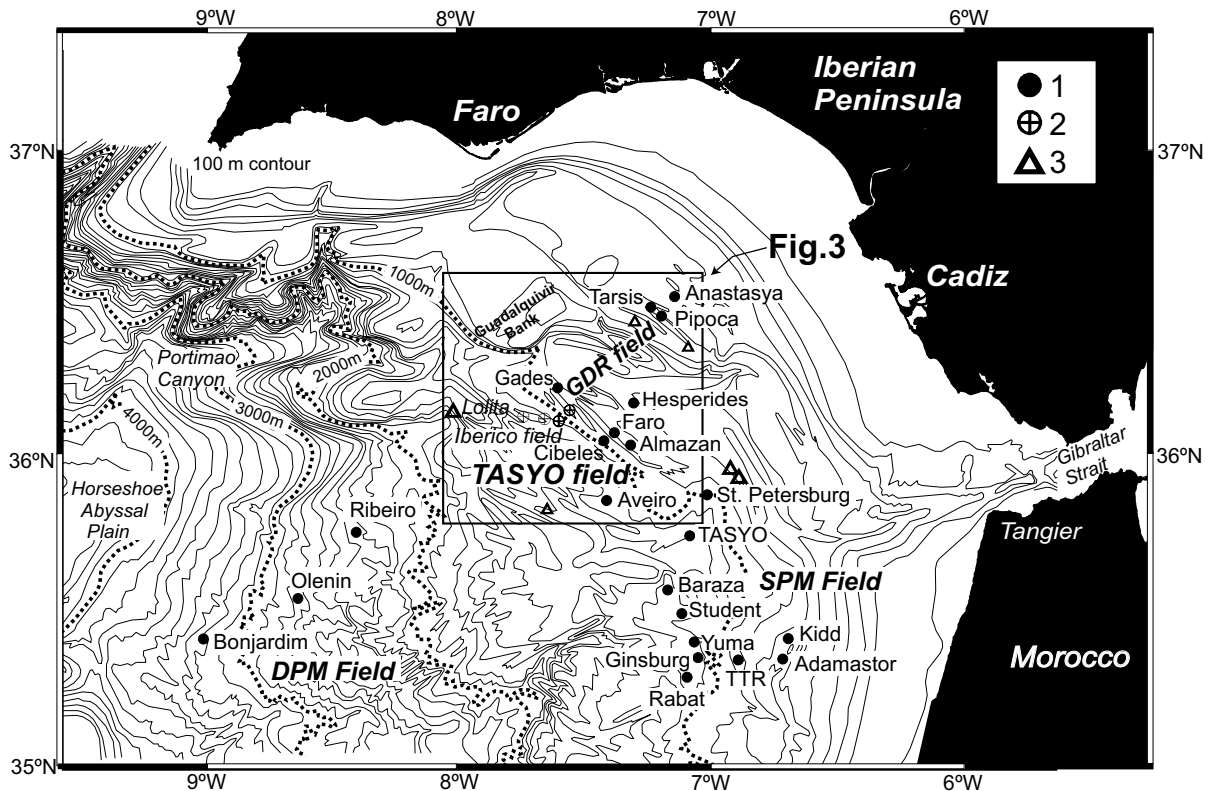


Fig. 2. Location and names of hydrocarbon seepages identified in the Gulf of Cádiz: 1 = mud volcanoes with sulphide mud breccias; 2 = mud cones with hydrocarbon-derived carbonate chimneys; and 3 = other circular features. See text for explanation and references. Box inset shows the location of multibeam mosaic of the study area shown in Fig. 3.

front of the Gibraltar arc, the westernmost tectonic belt of the Alpine–Mediterranean compressional system which has formed in response to the convergence between the African and Eurasian plates. The emplacement of allochthonous units took place in the Gulf of Cádiz during the Tortonian (ca 7.1–11.2 Ma) (Maldonado et al., 1999), as an accretionary wedge formed by the interaction of the Alboran Domain with the passive margins of the Eurasian and African plates (Flynn et al., 1996). Four main tectonic allochthonous provinces surround the internal zones of the Gibraltar arc orogenic belt, which overlies both the Iberian and African passive margins (Fig. 1). These include: (1) the flysch units of the Campo de Gibraltar complex; (2) the external zones, a tectonically detached Mesozoic sediment ranging from Lower Jurassic to Upper Cretaceous–Palaeocene pre-tectonic units; (3) the Triassic Diapir

Zone, composed mainly of salts, gypsum and shallow carbonate deposits emplaced as diapiric expulsion structures by thrusting of thick nappes of Mesozoic sediments (Berástegui et al., 1998); and (4) the front of a deformed wedge, mainly formed by plastic clays and marls of Early–Middle Miocene age (Maldonado et al., 1999).

The most frontal parts of the Gibraltar arc are composed of Triassic evaporites and Miocene plastic marls and have been referred to traditionally as the ‘Olistostrome Zone’ (Perconig, 1960–62) or ‘Gualdalquivir Allochthonous Unit’ (Blenkinship, 1992) (Fig. 1). Gibraltar arc emplacement ended during the Late Miocene, which coincides with accelerated tectonic subsidence on the shelf, resulting in gravitational gliding and spreading of Triassic salt and Miocene shale deposits towards the Central Atlantic basins (Somoza et al., 1999). Major gravitational gliding nappes,

which have been identified in the Gulf of Cádiz, on the Spanish–Portuguese margin (Cádiz Salt Nappe) and Moroccan margins, were detached from the front of the Gibraltar arc (Lowrie et al., 2000). Since the early Pliocene, the former plastic olistostrome mass, with a thickness exceeding 2.4 km, has extended from the shelf towards the Horseshoe and Seine abyssal plains, west of the Gibraltar arc (Torelli et al., 1997; Vázquez et al., 2001).

Deformation structures observed on migrated multifold seismic lines along the shelf and slopes of the Gulf of Cádiz provide geometric evidence for shale/salt tectonics and related hydrocarbon seepage on the sea floor (Baraza and Ercilla, 1996; Battista et al., 2000; Fernández-Puga et al., 2000; Somoza et al., 2001). Overpressure compartments generated beneath salt/shale wedges provide avenues for hydrocarbon gases, fluids (brine waters) and fluidised sediments to flow or seep upwards through contractional toe-thrust structures to form seepage-related structures on the sea floor (Lowrie et al., 1999).

3. Methods and data acquisition

The data presented in this paper were collected aboard R/V *Hespérides* and R/V *Cornide de Saavedra* between 1999 and 2001. Ship positioning was achieved with a differential Global Positioning System (DGPS) with an average navigational accuracy of better than ± 5 m. Swath bathymetry was collected on the R/V *Hespérides* using the Simrad EM12S-120 system, a hull-mounted multi-beam echo-sounder. More than 1200 km of new data were obtained during the TASYO-2000 cruise. The total area mapped was 8500 km². The EM12S-120 system operates at a main frequency of 13 kHz, with 81 beams, which allow a maximum coverage angle of 120° (about three times the water depth). This system, triggering with a range of pulse lengths from 2 to 10 ms, has a vertical resolution of 0.6 m. Temperature measurements of the water column were made with a precision of $\pm 0.15^\circ\text{C}$. Problems encountered during bathymetric data processing have been attributed to the sharp temperature differ-

ence between the warm Mediterranean Outflow Water (MOW) and overlying cool Atlantic surface waters. Preliminary processing of the data was done onboard using Simrad Neptune software. A bathymetric map, contoured at an interval of 10 m, and a sea-floor backscatter image were generated (León et al., 2001).

The upper sediment column and sea floor were studied using high (3500–7000 J Sparker system, 50 Hz to 4 kHz) and ultra-high resolution (15–18 kHz) chirp seismic methods. Shallow high-resolution sediment echo-sounding data were acquired with a parametric narrow-beam sub-bottom profiler TOPAS (Topographic Parametric Sound) onboard the R/V *Hespérides*. TOPAS uses chirp wavelets, operating at two simultaneous primary frequencies, 15 and 18 kHz. Through the parametric effect in the water, a secondary frequency is produced in the range of 0.5–5 kHz. Penetration of up to 100 m was obtained with a resolution of 0.5–1.0 m. Analogue plots were available for preliminary interpretation onboard. Digital data were recorded using Delph2 Triton software and preserved on magnetic disk. These data were studied post-cruise in more detail after further processing techniques were applied. A dense network of Sparker seismic data was collected during cruises Anastasya-99 and Anastasya-00 with an energy source ranging between 3500 and 7000 J and a recording length of 2 s TWT (two-way travel). Pre-processing of digital data was performed using Delph2 software.

Standard gravity cores (3 m in length) were collected from selected mud volcanoes identified on the bathymetric and backscatter maps. A rectangular benthic-type dredge was used when carbonate slabs impeded the penetration of gravity cores. A narrow-beam echo-sounder was also used during dredging operations.

4. Results

Multibeam bathymetry of the study area (Fig. 3) shows two linear ridges, the Guadalquivir Diapiric Ridge (GDR) and Cádiz Diapiric Ridge (CDR). The crest of the GDR occurs in water depths ranging from 380 to 940 m below the sea

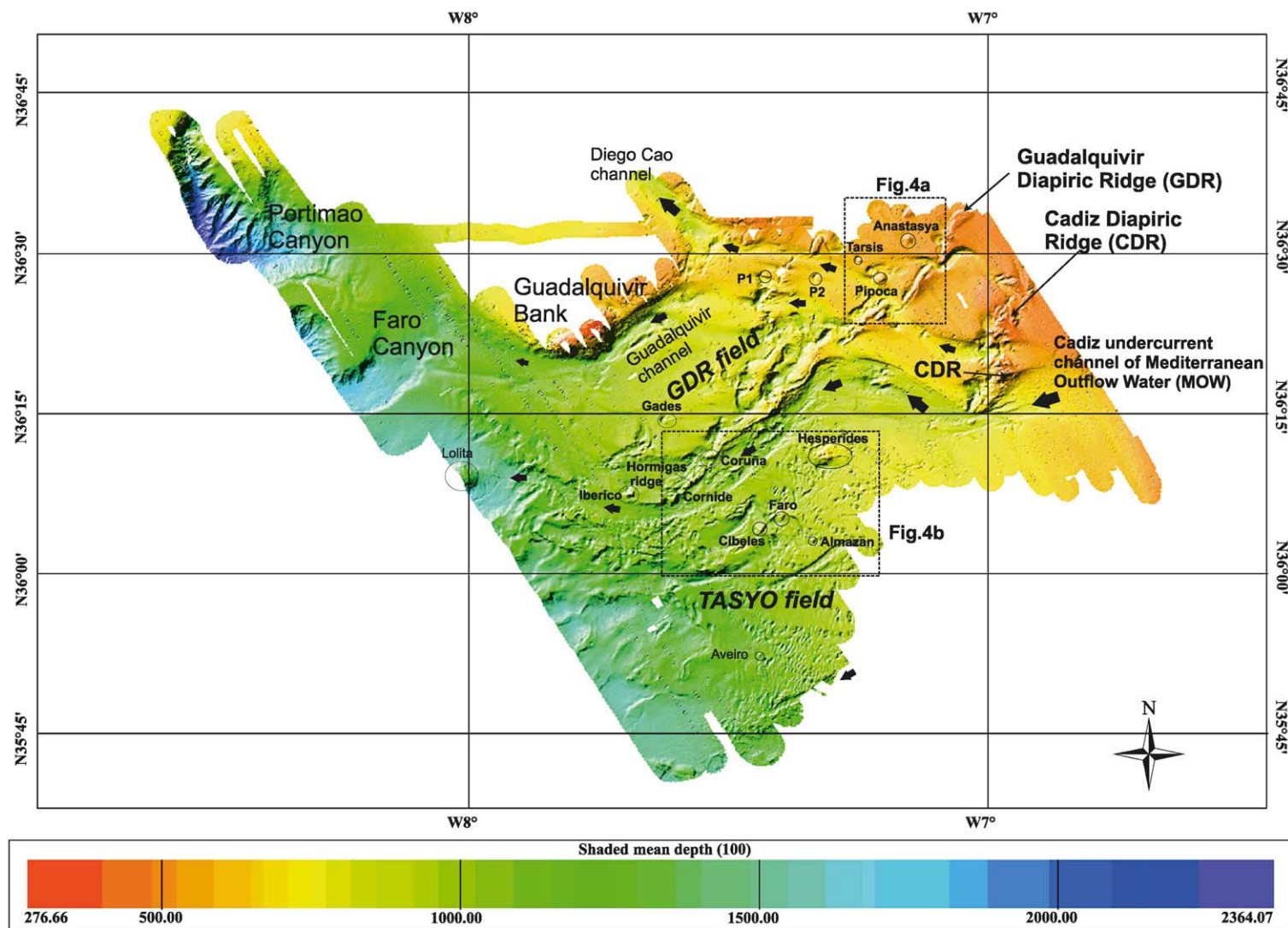


Fig. 3. EM12 multibeam bathymetry relief of the study area during the *Hesperides* cruise TASYO-2000. Illumination is from the northwest. Guadalquivir Bank (Paleozoic and Mesozoic Iberian basement); the Guadalquivir and Cádiz Diapiric Ridges (GDR and CDR) formed by Early–Middle Miocene plastic marls of the olistostrome; the Mediterranean Outflow Water (MOW) undercurrent channels: Cádiz, Guadalquivir and Diego Cao; and the submarine canyons of Portimao and Faro. Circles show the location of sub-circular features interpreted as mud volcanoes and mud cones subdivided in the TASYO and GDR fields as described in the text. Box inset shows location of detailed multibeam bathymetry of single mud volcanoes in the GDR field (Fig. 4a) and the TASYO field (Fig. 4b).

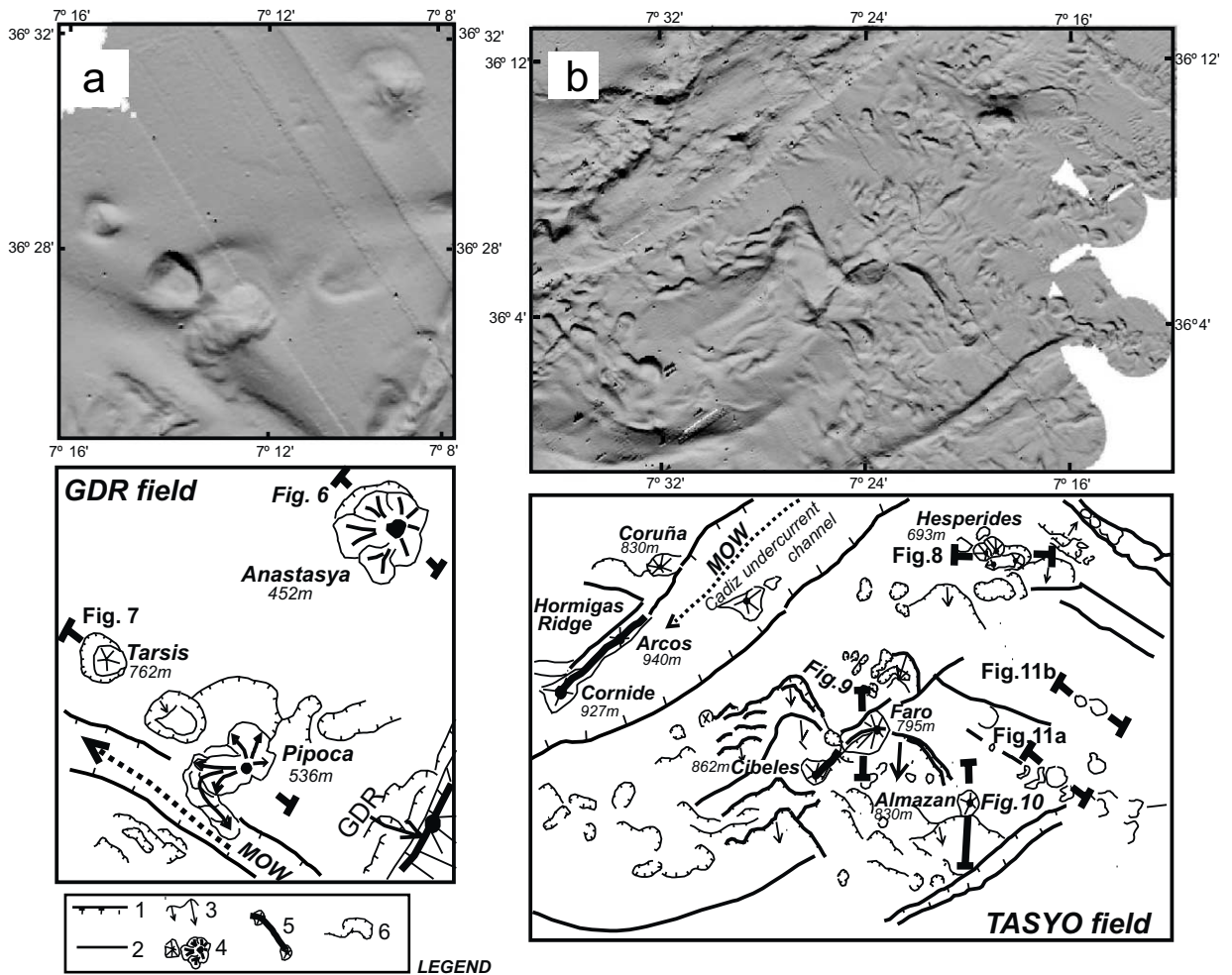


Fig. 4. Detailed multibeam relief and location of seismic profiles of the northeastern part of the GDR field showing the Anastasya, Pipoca and Tarsis mud volcanoes (a). MOW = Mediterranean Outflow Water. (b) The TASYO field showing a characteristic relief formed by a multitude of crater-like depressions and large slide scars. Legend: 1 = contourite channel scarp; 2 = fault evidence on sea floor; 3 = slide scar; 4 = mud volcano; 5 = mud cones allineated in a mud ridge; 6 = circular depression.

surface and is approximately 85 km long, 4000 m wide and has an overall relief of 250 m. The crest of the CDR ranges from 370 to 700 m below the sea surface, is approximately 27 km long, 4500 m wide, and has a relief of 300–250 m. On the bathymetric map, circular structures appear as topographic highs surrounded by moats (Fig. 4a). These features are observed on both sides of the diapiric ridges and are arranged into two main fields (Fig. 3): the GDR field, at the north-western edge of the GDR, and the TASYO field on the south side of the Cádiz undercurrent chan-

nel. Table 1 summarises the morphology of these mound structures.

Along the GDR field (Fig. 3), four mounds were identified as mud volcanoes (Anastasya, Tarsis, Pipoca and Gades mud volcanoes), and are characterised by the presence of mud breccia deposits with a strong H_2S smell. Two similar features, having positive topographic relief and a circular, conical shape, were also identified, P1 and P2 (see Table 1), but no sediment samples were acquired. The westernmost part of the GDR, between 8° and 7°40'W, is characterised

Table 1
Summary of the morphology, acoustic characteristics and sedimentary nature of the subcircular elevated sea-floor structures related to hydrocarbon fluid venting

Name	Depth (m)	Relief (m)	Shape	D-max (km)	D-min (km)	Aspect ratio	Profile structure	Slope gradient	Acoustic characteristics	Sample ref.	Sedimentary summary	Interpretation
<i>GDR field</i>												
Anastasya	452	80	Sub-rounded with asymmetric collapse rim	1.5	1.1	0.73	Flat-topped cone	6°–8°	High reflectivity surface	00-TG5	'Mousse-like' muds with high gas saturation and strong H ₂ S smell on the top. Mud breccias of heterometric clasts (limestones, sandstones and blue marlstone) on the flanks covered by 5 cm recent sands	Single mud volcano
									Transparent facies interfingering with coherent reflectors form 'barrel-like' edifice	00-TG6		
										00-TG7		
										00-TG8		
										01-TG2		
Pipoca	536	97	Sub-rounded with asymmetric collapse rim (2 km in diameter)	2.1	1.5	0.71	Flat-topped cone	3°–7°	High reflectivity surface	01-TG1	Mud breccia with layers of ahermatypic corals and bivalvs, overlaid by 35 cm of brown coarse-grained sands	Single mud volcano
									Transparent facies interfingering with coherent reflectors form 'barrel-like' edifice	01-TG3		
										01-DA12		
Tarsis	762	60	Sub-circular with asymmetric collapse rim	0.9	0.8	0.88	Flat-topped cone	6°–8°	Flat-topped cone with high reflectivity surface			Single mud volcano
									Transparent facies interfingering with coherent reflectors			
P-1	670	65	Oval-round	0.8	0.73	0.91	Flat-topped cone	8°–10°	Transparent facies interfingering with coherent reflectors			Possible mud volcano
P-2	737	87	Oval-round	1.3	1.0	0.76	Flat-topped cone	9°–12°	Transparent facies interfingering with coherent reflectors			Possible mud volcano
Gades	915	52	Round	0.9	0.9	1/C >	Asymmetric cone-shaped mound	5°	Transparent acoustic facies	01-TG4	Mud breccia overlaid by 3 m of oxidised (contourite) muds	Mud cone
Coruña	830	233	Asymmetric mound	–	–	–	Cone-shaped with asymmetric flanks	25°–30°	High-reflective surface	01-DA15	Carbonate chimneys and crusts. Muds with ahermatypic corals	Mud cone
									Chaotic to indistinct reflector on the subsurface			
Arcos	916	55	Round	–	–	–	Cone-shaped with asymmetric flanks	25°–30°	High-reflective surface	01-DA18	Carbonate chimneys and slabs	Mud cone
									Chaotic to indistinct reflector on the subsurface			
Cornide	927	255	Triangle	–	–	–	Cone-shaped with asymmetric flanks	5°	High-reflective surface	01-TG6	'Mousse-like' muds with carbonate chimneys, crusts and slabs	Mud cone
								15°–25°	Chaotic to indistinct reflector on the subsurface	01-DA1		
										01-DA2		

Table 1 (Continued).

Name	Depth (m)	Relief (m)	Shape	D-max (km)	D-min (km)	Aspect ratio	Profile structure	Slope gradient	Acoustic characteristics	Sample ref.	Sedimentary summary	Interpretation
Iberico	870	165	Oval-triangle	1.6	1.3	0.72	Cone-shaped with asymmetric flanks	22°–25°	Chaotic to indistinct reflector on the subsurface	00-DA10	Carbonate chimneys and slabs	Mud cone
Lolita	1560	316	Round	5.7	5	0.87	Cone-shaped	15°–20°	High-reflective surface	Ivanov et al. (2001)	Hemipelagic muds	Mud diapir
<i>TASYO field</i> Hespérides complex			Six single cones over an oval plateau	3	2.1	–	–	–	Strong reflectivity on the surface. Chaotic reflectors on the subsurface	00-DA12	Mud breccia (blue marlstones), carbonate crusts and calcite chimneys, Pogonophora sp., tubeworms and pyrite crystals	Mud volcano system associated with sea-floor piercing diapirism
H1	727	105	Round	1	0.85	0.85	Cone-shaped mound	9°–12°		01-DA5 01-DA6 01-DA7 00-TG10	Mud breccia and carbonate crusts	Single cone mud volcano
H2	682	150	Round	1.1	0.9	0.81	Cone-shaped mound	9°–12°		00-TG11	Mud breccia and carbonate crusts	Single cone mud volcano
H3	705	130	Round	1.1	0.7	0.63	Cone-shaped mound	9°–12°				Single cone mud volcano
Faro	795	190	Oval with collapse rim	2.6	1.8	0.69	Cone-shaped mound	8°–12°	High-reflective surface	01-TG14	Mud breccia of blue marlstone clasts with strong H ₂ S smell. Carbonate clasts on the top. 10 cm of oxidised sands	Mud volcano related to slide scars and collapse structures
Ciboles	860	150	Oval-triangle	1.2	0.9	0.75	Asymmetric cone-shaped mound	3°–5°	Short feeder channelled with a diameter (1 km) linked to a cone-like structure of chaotic reflectors	00-TG9	Mud breccia and carbonate crusts and slabs	Mud volcano related to slide scars and collapse structures
Almazán	870	75	Round	1.5	1.2	0.73	Cone-shaped mound	12°–15° 8°–12°	Feeder channel composed of chaotic to indistinct reflectors	01-TG8	Mud breccia of blue to grey marlstone with strong H ₂ S smell interbedded with fluidised 'mousse-like' muds. Layers with abundant aberrant corals and bivalvs. 15 cm of oxidised sands	Mud volcano associated with diapirism, slide scars and collapse structures
Aveiro	1180	110	Round	0.9	0.85	0.94	Cone-shaped mound	9°–13°	Chaotic to indistinct reflectors	Ivanov et al. (2001)	Mud breccia	Mud volcano associated with collapse structures

See Fig. 3 for location.

by an arcuate-shaped ridge, formed by a series of prominent mounds which bound the Cádiz undercurrent channel. Three large mounds, named Iberico, Cornide, and Coruña, exhibiting high positive relief (~ 250 m), were identified along this arcuate ridge named Hormigas (Fig. 3). At their western end, we also observed, in the multibeam bathymetry, the largest circular structure of the region, named Lolita. This structure was sampled during the TTR-11 cruise and has been interpreted as a mud cone due to the absence of mud breccia.

On the south side of the Cádiz undercurrent channel, the detailed bathymetric map revealed the probable presence of numerous mud volcanoes, the presence of large pockmark craters, and a feature resembling the scar of a large sediment slide that has transported material towards the Horseshoe abyssal plain (Fig. 4b). This area, named the TASYO field, extends from $36^{\circ}15'N$ $7^{\circ}W$ to $35^{\circ}45'N$ $7^{\circ}30'W$, and is characterised by an irregular, hummocky sea floor defined by the presence of numerous circular to oval, crater-like features alternating with features exhibiting positive topographic relief. Depths range from 750 m on the top of cone-shaped structures to 1050 m on large crater-like depressions. Several channels are observed crossing the TASYO field in a SW direction parallel to the Cádiz undercurrent channel. Five large mud volcanoes were identified in the TASYO field (Aveiro, Hespérides, Cibeles, Faro and Almazán). In addition, more than 30 sub-circular structures can be observed on the detailed bathymetric map of the TASYO field (Fig. 4b).

5. Morphology and nature of deposits

All of the sea-floor structures observed in the Spanish–Portuguese margin can be divided according to their morphology and nature of deposits (Fig. 5): (i) circular-shaped mud volcanoes; (ii) plateau-type complex systems, composed of several circular-shaped mud volcano cones; (iii) sub-rounded to oval mud volcanoes; (iv) rounded crater-like depressions with small cone-shaped domes at their centre; (v) mud cones with carbonate chimneys.

5.1. Single circular mud volcanoes

Along the northern edge of the GDR, a series of wide, sub-circular mounds surrounded by ring-shaped sea-floor depressions (moats) are observed on the bathymetric map (Fig. 4a). The moats are approximately 60 m deep. These mounds were imaged with seismic data and sampled with gravity cores. The main structures are named Anastasya, Tarsis, Pipoca and Gades. P1 and P2 are lower relief mounds and are well represented in the bathymetric data (Fig. 3).

The most prominent structure is Anastasya mud volcano (Fig. 5a), a 80 m cone-shaped mound, 1.5 km in diameter with its top at 452 m water depth. The regular cone shape of this mud volcano is symmetrical, with slopes between 6° and 8° . In the centre of the volcano is a small flat-topped, dome-like feature (about 350 m in diameter) with steep slopes of 10° – 13° (Fig. 6). Gravity cores collected from the top of this mud volcano (cores 01-TG2 and 00-TG5) yielded very plastic ‘mousse-like’ muds with high-gas saturation and a strong H_2S smell, thinly covered (5 cm) by Recent medium-grained sands. Along the flanks of the volcano, polygenic sulphide mud breccia were recovered from three gravity cores (00-TG6, 00-TG7 and 00-TG8). These mud breccias are composed of heterometric clasts of limestones, sandstones and blue mudstones. Authigenic pyrite nodules more than 1 cm in diameter were collected from the sulphide mud. Mud breccia deposits are covered by 15 cm of brown muds. The seismic character of the Anastasya mud volcano exhibits strong surface and transparent to chaotic reflectors in the inner part of the edifice. Transparent seismic facies form ‘barrel-like’ edifices beneath the sea floor, a seismic characteristic of a large number of sub-bottom mud volcano structures (Ivanov et al., 1996). Transparent facies interfinger with adjacent coherent reflectors of the host sediment, which consists of sequences of mud and sand contourite deposits (Nelson and Maldonado, 1999). Some of these coherent reflectors bend slightly downward, and can be correlated with major discontinuities within the contourite deposits (1 in Fig. 6). Overlying these depressed reflectors appear cone-shaped transparent facies

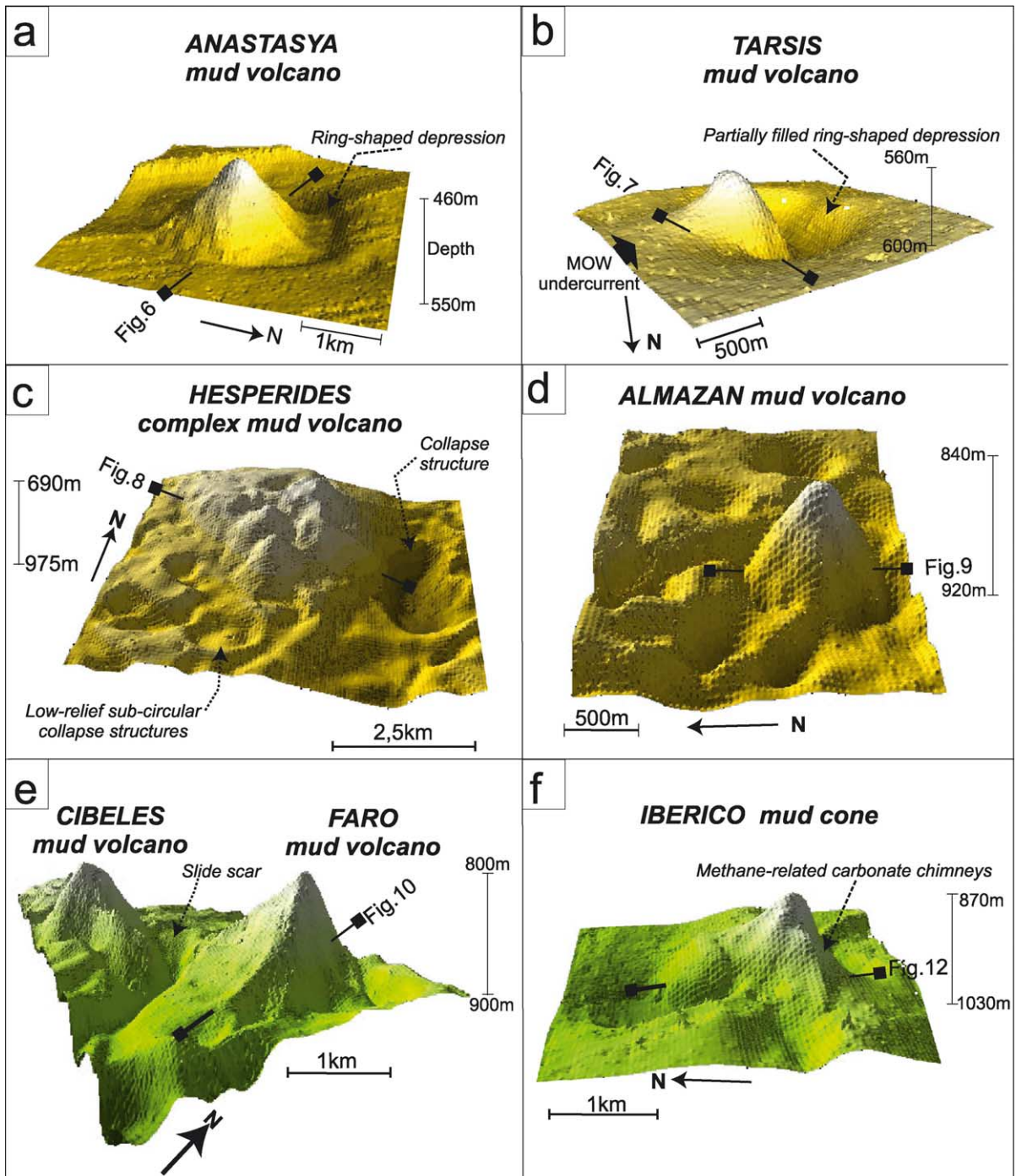


Fig. 5. 3D images from multibeam bathymetry showing the different types of morphologies related to hydrocarbon seepage. (a,b) Single circular mud volcanoes (Anastasya and Tarsis). (c) Multi-cone mud volcano (Hespérides). (d,e) Oval mud volcanoes (Faro, Cibeles and Almazán). (f) Mud cones with methane-related carbonate chimneys (Ibérico). Location of seismic lines across these features is also shown.

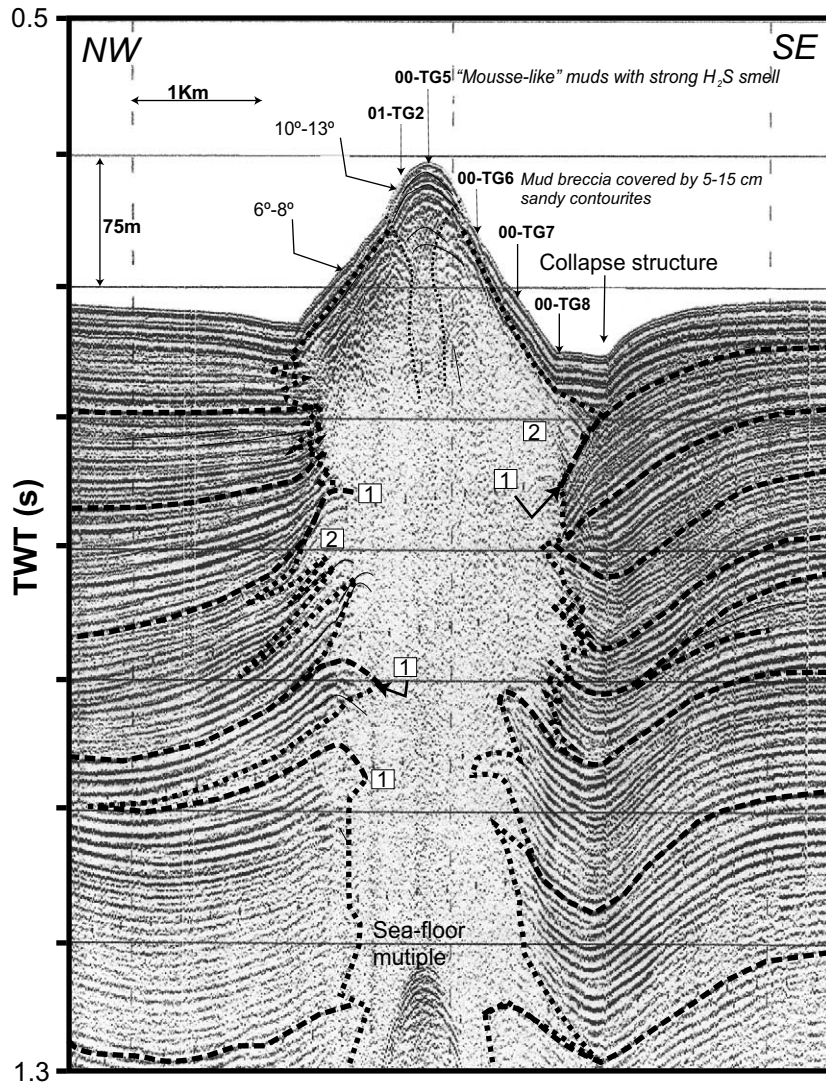


Fig. 6. Single-channel sparker line across the Anastasya mud volcano with location of gravity cores. 1 = Downward bending of reflectors that continue as major discontinuities along the contourite deposits; 2 = transparent facies interfingering with adjacent coherent reflectors. Note the small flat-topped dome at the centre of the mud volcano, formed by 'mousse-like' muds. The collapse structure is observed on multibeam bathymetry as a ring-like depression (see Fig. 5a). For location, see Fig. 4a.

(2 in Fig. 6), which are, at the same time, overlapped by high-reflective units. The collapse depression surrounding the Anastasya mud volcano is illustrated on multibeam bathymetry, and is depicted in the seismic profile as downward-bent sub-bottom reflectors.

The Pipoca mud volcano is morphologically similar to Anastasya, and appears in the multibeam bathymetry data as a sub-rounded cone-

shaped feature, with maximum diameter of 2.1 km, a relief of 97 m and the summit occurs at 536 m water depth. Several lobes formed by successive mud flows can be identified on the southwestern slope of this mud volcano (Fig. 4). The flanks are asymmetric, with gentle slopes ranging between 3° and 7° on the southernmost part, where the mud flows are located, and between 11° and 12° on the northern flank, which faces a

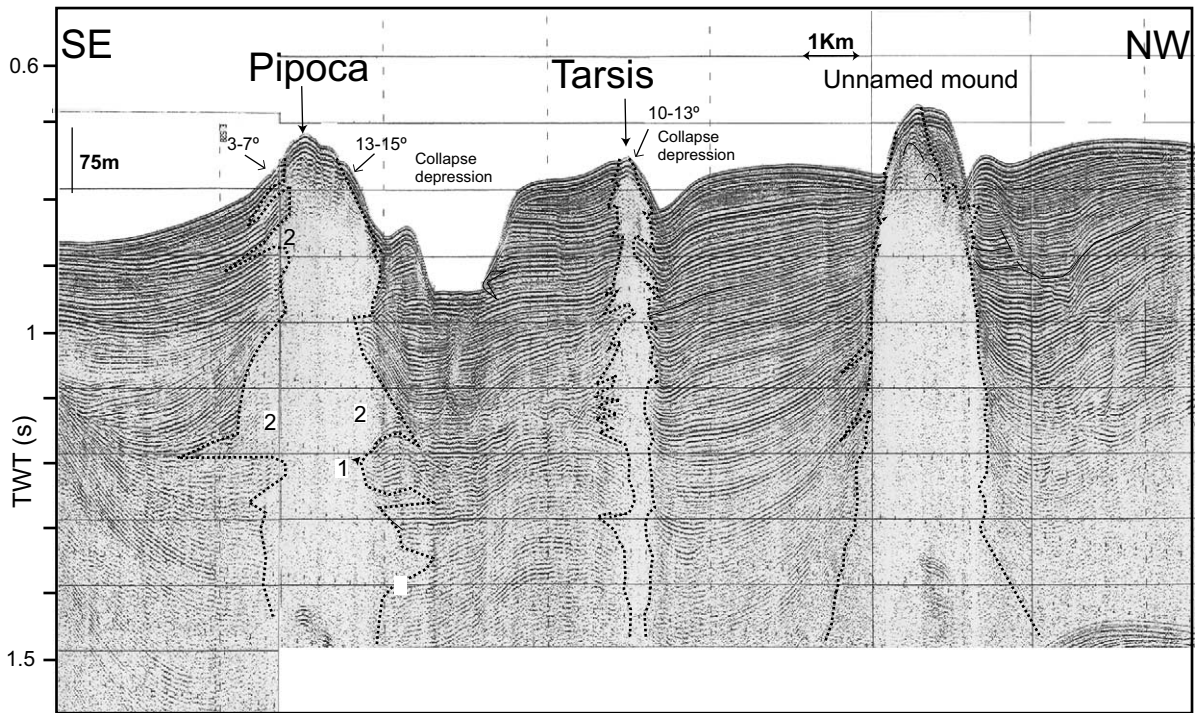


Fig. 7. Single-channel sparker line across the Tarsis and Pipoca mud volcanoes with location of gravity cores. 1=Downward bending of contourite reflectors are also observed on the base of the cone; 2=major discontinuities of the contourite host sediments that are correlated with the base of interfingering of the mounded transparent facies-shaped transparent mounds. For location, see Fig. 4a.

large ring-shaped depression (Fig. 7). This depression, with a diameter of 2 km, has very steep walls with slopes ranging from 25° to 30°. Gravity cores taken in the crest of this mud volcano (cores 01-TG1 and 01-TG3) yielded mud breccia deposits overlain by a layer of ahermatypic corals and bivalves. The mud breccia and coral deposits are overlain by 35 cm of brown coarse-grained sands with abundant coral and bivalve debris, which have been interpreted as recent contourite deposits.

The Tarsis mud volcano (Fig. 5b) is NW of Pipoca, occurs at 762 m water depth, is a low-relief mound that is surrounded by a ring-shaped moat. Its diameter at the seabed is 0.9 km and its height is 60 m. The flanks are rather asymmetric, like the Pipoca mud volcano, with a southern slope ranging from 6° to 8° and a northern flank with slopes up to 13°. The southern flank appears to be slightly smoothed by contourite deposits,

whereas the northern flank has a sub-circular depression. Sub-bottom seismic expression of the Pipoca and Tarsis mud volcanoes shows the same type and sequence of acoustic facies as those identified in Anastasya. Along a seismic line crossing the axes of Pipoca and Tarsis cones, at least seven discontinuities of the contouritic host sediments may be correlated with interfingering transparent facies which form cone-shaped edifices (Fig. 7). Collapse depressions appear on their northern flanks and appear in seismic data as downward reflections of the contouritic sequence. Even though acoustic anomalies and blanking zones may be identified beneath the sub-circular depressions, there is no evidence of gas seepage.

5.2. Complex mud volcano with numerous cones

The Hespérides mud volcano is the largest

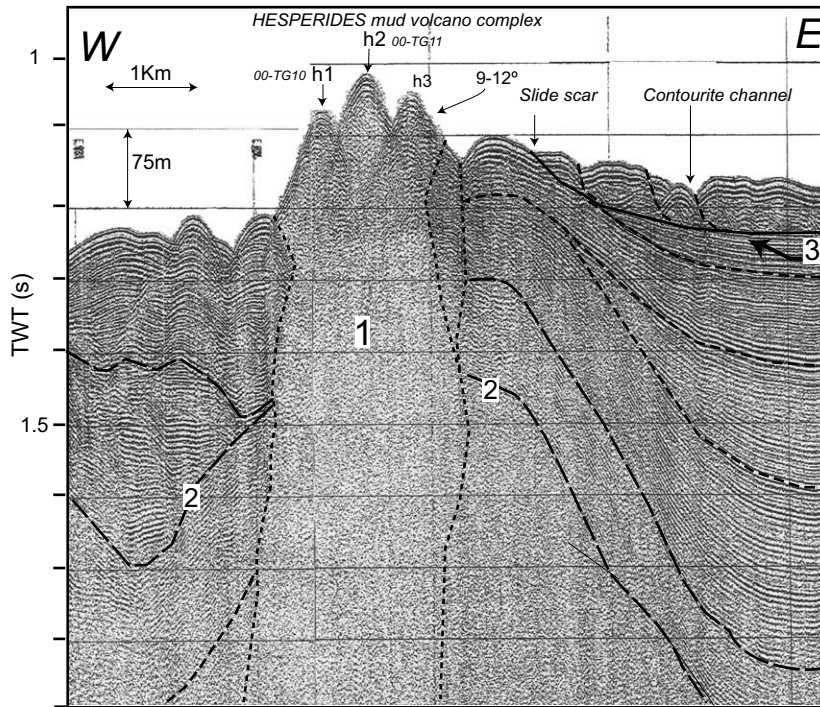


Fig. 8. Single-channel sparker line across the Hespérides mud volcano complex formed by single circular cones (h1, h2 and h3); 1=chaotic reflectors on their subsurface that deform the: 2=adjacent reflectors of the contourite host sediments and form low amplitude folds on the sedimentary basin; 3=discontinuity at the base of a slide observed on multibeam bathymetry (see Fig. 4b), disturbing the reflectors of the uppermost contourite deposits.

structure in the TASYO field. This mud volcano is composed of numerous cones with a seabed diameter of more than 3 km and a relative height of 150 m (Fig. 4b). Detailed multibeam bathymetry shows six single circular cone-shaped domes, with seabed diameters ranging from 1.1 to 0.4 km (Fig. 5c). Flanks of all single cones are steep (8–12°) relative to the single mud volcanoes described above. Several sea-floor features suggesting instability surrounding the mud volcano may also be identified on the multibeam bathymetry. A major oval, crater-like collapse structure, forming a depression below the surrounding sea floor of 2 km in diameter and having steep slopes of up 25°, is located at the southeastern side of the Hespérides complex (Fig. 5c). In addition, several slide scars are also observed.

The acoustic character of the Hespérides mud volcano exhibits strong reflectivity on the surface and chaotic reflectors in the subsurface (Fig. 8), in

contrast to the non-reflective, transparent facies observed on the single mud volcanoes described above. Seismic lines crossing this complex show a cone-shaped structure, which consists of chaotic facies that deform adjacent reflectors of the contourite host sediments. This structure rises from 1.9 s TWT (which is the penetration limit of the seismic source) to 1.2 s TWT, forming low amplitude folds on the adjacent sedimentary basin. On the surface, a major slide, which appears in the multibeam bathymetry, is observed on the eastern side of the Hespérides complex. A detached layer at about 1.2 s TWT involves a thickness of 50–80 ms TWT of disturbed contourite deposits.

Cores (00-TG10, 00-TG11) and dredge samples (00-DA12, 01-DA5, 01-DA6, 01-DA7) collected from the crest of the single cones (Fig. 8) of the Hespérides complex yielded large amounts of brown carbonate crusts and chimneys and a polygenic matrix breccia with a strong H₂S smell.

Gravity cores show mud breccia deposits covered by only 5 cm of sandy sediments which are bioturbated and show evidence of oxidation. The mud breccia consists mainly of heterometric and large clasts (up to 5 cm) of blue marlstone. This type of sediment is characteristic of the Early to Middle Miocene pre-olistostromic unit M1 (Maldonado et al., 1999). Pogonophora tubeworms and pyrite were also collected from the matrix of the breccia, all characteristics of chemosynthetic communities. Carbonate crusts and chimneys located at the surface of this mud volcano, collected by dredging, consist of calcite (40% CaO, 13.5%, 10.7% Fe₂O₃ and 1.6% MgO), and minor proportions of Fe dolomite, in contrast to other methane-related carbonate chimneys and crusts discovered in the Gulf of Cádiz, which are mainly formed by ankerite carbonates (Díaz del Río et al., 2003). Dredge samples from the bottom of the large crater-like collapse structure adjacent to the Hespérides complex revealed mud deposits without evidence of gas-rich sediments or carbonate crusts on its surface.

5.3. Oval mud volcanoes associated with slides

Three oval mud volcanoes have been surveyed on the TASYO field and are named Faro, Cibeles and Almazán. All of these structures are arcuate in shape, 8 km in diameter, and with prominent slopes up to 25° (Fig. 4b). The Cibeles and Faro mud volcanoes are located along the northwestern side of a ridge, whereas the Almazán scar is at its westernmost edge. This ridge has a positive relief of more than 275 m between Cibeles and Faro cones, but transforms to a deep depression more than 125 m below the adjacent seabed at the westernmost side of the ridge between Faro and Almazán mud volcanoes.

The largest mud volcano, the Faro mud volcano, appears on multibeam bathymetry as an oval-shaped feature with a maximum seabed diameter of 2.6 km, oriented NNW–SSE, and exhibits 190 m of bathymetric relief (Fig. 5e). Seismic lines reveal that it has a cone-shaped profile, with high acoustic backscatter from its surface (Fig. 9). Faro has an asymmetric form, with steep slopes of 12° on its northern side and 8° on its

southern side. The sub-bottom expression of the cone is identified on seismic lines as a chaotic reflector, showing clearly a widening of the feeder channel at its base (Fig. 9). The feeder channel has a sub-sea-floor diameter of 1 km beneath the base of the mud volcano. This feature is linked with a cone-like structure of chaotic and indistinct seismic reflection patterns, which flexures and forms low-amplitude folds in adjacent well-stratified sediments. High-angle normal faults are also identified on the top of this structure. At the surface, small slides are identified at about 150 ms TWT beneath the sea-floor surface, and are identified on seismic lines at both sides of this cone. These features are observed as listric normal faults deforming the upper sedimentary sequence. A minor cone-shaped mound is also identified in the south, with a very low positive relief and a narrow feeder channel, with a sub-sea-floor diameter of 0.4 km that cuts through the adjacent sedimentary sequence. Even though this structure was not sampled, its acoustic response, cone shape and the existence of a feeder channel suggest that it may also be a mud volcano (Fig. 9). Gravity cores from the crest of the Faro mud volcano (core 01-TG14) yielded 50 cm of mud breccia with a strong H₂S smell covered by 10 cm of oxydised brown sands. Carbonate clasts at the boundary between the mud breccia and the upper recent marine sediments suggest the existence of carbonate crusts on this mud volcano. Mud breccia show heterometric clasts composed of sandstones, limestones and marlstone and some blue marlstone clasts up to 5 cm in diameter. The redox potential ranges from –280 mV at 60 cm below sea floor to –170 mV at the boundary between mud breccia and oxydised sands.

The Cibeles structure, which lies southwest from the Faro mud volcano, shows similar features (Fig. 5e). It appears as an oval-shaped feature located at 860 m water depth with a maximum seabed diameter of 1.2 km in the NW–SE direction and a relief of 150 m above the surrounding irregular sea floor. The cone shows an asymmetric profile with steep slopes of 12°–15° on its eastern flank and smooth slopes of 3°–5° on the western flank. A gravity core taken at the crest of this mud volcano (core 00-TG9) recov-

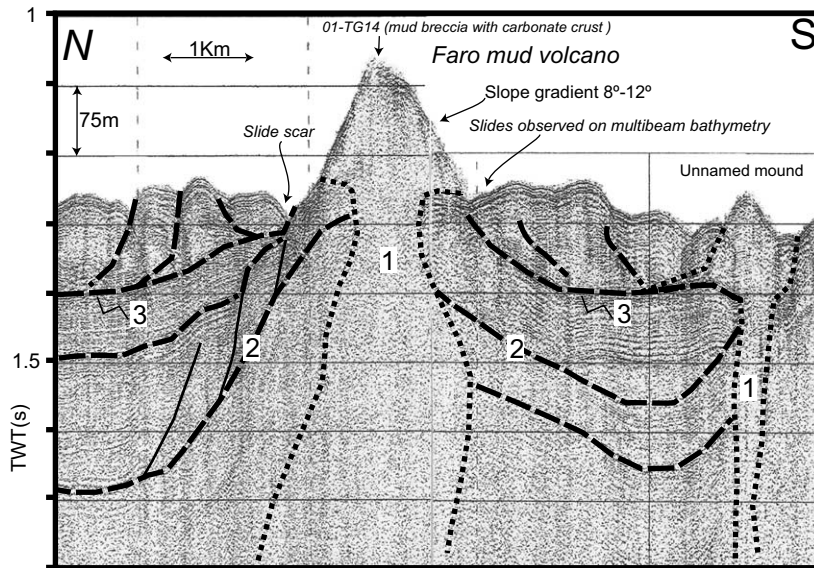


Fig. 9. Single-channel sparker line across the Faro mud volcano. The sub-bottom expression of this structure shows: 1 = conic-like disturbance with chaotic and indistinct seismic reflection patterns, narrowing upwards (feeder channel?) and linkage with the base of the mud volcano; 2 = low-amplitude folds of overall adjacent well-stratified sediments. High-angle normal faults are also identified on the top of this structure. 3 = Detached layers of the slides which superficial expression is well observed on multibeam bathymetry (see Fig. 4b). Note a small mound observed to the south of the line with the same acoustic characteristic as the Faro mud volcano.

ered 15 cm of oxydised brown muddy sands overlying grey clay muds with obvious indications of gas saturation: degassing structures and a strong H_2S smell.

The Almazán mud volcano, in the easternmost part of the slide structure, has a morphology similar to the above types. It appears as an oval mound with a maximum seabed diameter of 1.5 km along the NNW–SSE direction and a minimum diameter of 1.2 km along the orthogonal direction (Fig. 5d). The cone, with a relief of 75 m above the surrounding sea floor, has a symmetrical profile, whose flanks have steep slopes ranging from 8° to 12° (Fig. 10). High-reflectivity coherent reflectors characterise the surface of the cone whereas chaotic to indistinct seismic reflection patterns form the inner parts of the edifice. The mud volcano feeder channel is expressed on the seismic section in the form of a columnar disturbance with chaotic and indistinct seismic reflection patterns that cut well-stratified sedimentary sequences. The feeder channel has an average diameter of 600 m and can be traced to a depth of

at least 700 ms TWT below the crest of the mud volcano (Fig. 10). Another feeder channel with similar characteristics but without superficial expression can be identified on sparker seismic lines. Moreover, blanking zones without acoustic response are identified on the shallowest sediments, and are probably linked to these feeder channels (Fig. 10). A gravity core from the crest of the Almazán mud volcano (core 01-TG8) yielded 90 cm of a heterometric mud breccia with a strong H_2S smell, covered by 15 cm of coarse-grained bioclastic sands. The top of the mud breccia shows abundant bioturbation and gastropods with evidence of oxidation processes. Layers with abundant ahermatypic corals and bivalves are interbedded between mud breccia deposits. Clasts are mainly centimetre-sized blue to grey marlstone. ‘Mousse-like’ muds appear also interbedded within the mud breccia deposits. The redox potential measured at the bottom of the core is -270 mV, whereas at the top of the mud breccia it is only -81.7 mV, which is similar to the sea floor.

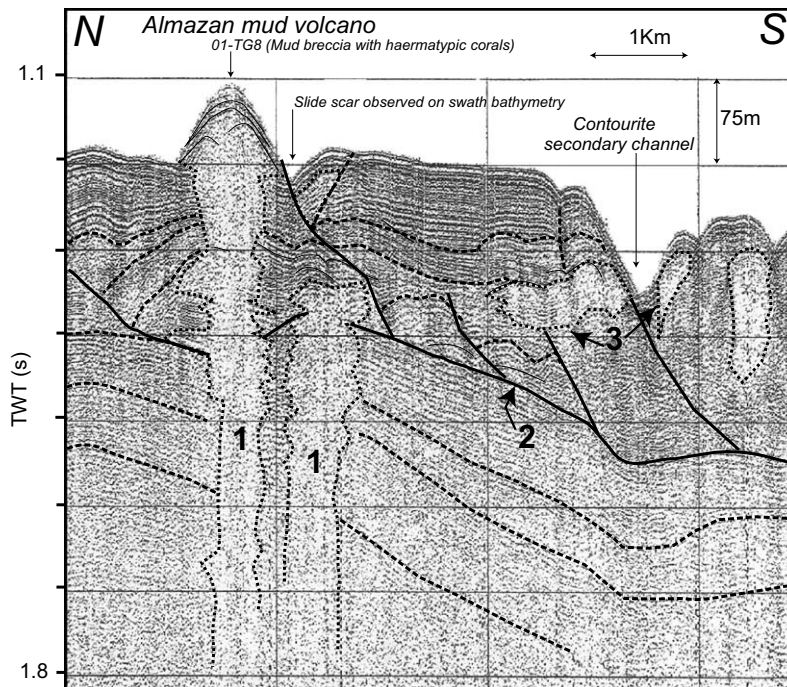


Fig. 10. Single-channel sparker line across the Almazán mud volcano: 1 = feeder channel showing columnar disturbance with chaotic and indistinct seismic reflection patterns that cut well-stratified sedimentary sequence; 2 = major southward-dipping discontinuity reflected on the sea-floor morphology as a major slide scar (see also Fig. 4b); 3 = chaotic and indistinct seismic reflection patterns interbedded with disturbed reflectors interpreted as fluidised sediments by rising fluids that may be stored in the superficial permeable sediments beneath the sea floor in levee or contourite channels. For location, see Fig. 4b.

5.4. Low-relief mounds and crater-like depressions

More than 30 circular crater-like depressions can be observed on the detailed bathymetric map in the TASYO field (Fig. 4b). The seabed diameter of these structures varies between 800 and 1200 m, with steep slopes ranging from 25° to 30°. The internal structure of these features was resolved with ultra-high resolution seismic methods (TOPAS). Two main types of circular structures can be distinguished on the seismic lines (Fig. 11): low-relief mounds and crater-like collapse structures.

Ultra-high resolution seismic data of the circular depressions observed on the multibeam bathymetry map (Fig. 4b) revealed the presence of small cone-shaped mounds with very low relief (10–15 m). These small mounds show step-like profiles and benches along their slopes (Fig. 11a). The internal acoustic response in the inner parts of the mound is transparent, whereas highly

reflective facies are found at the top, similar to those observed in larger mud volcano structures. The maximum diameter of the mounds at the sea floor is about 500 m. However, seismic profiles show that transparent acoustic facies beneath the sea-floor mounds extend more than 2 km from their axis, forming a conical structure with thicknesses ranging from 70 ms TWT along its axis, decreasing to 20 ms TWT on the border. The feeder channel is observed in the form of columnar transparent seismic reflection patterns that break the adjacent well-stratified sediments (Fig. 11a). Downward dip of the host sediment reflectors towards the conduit is also distinguished.

Crater-like depressions with steep slopes (up to 25°) show seabed diameters of 1–1.2 km. These depressions are similar to pockmarks as described by Hovland and Judd (1988) and Kelley et al. (1994). In the centre of these depressions, a seismic section shows feeder channels in the form of

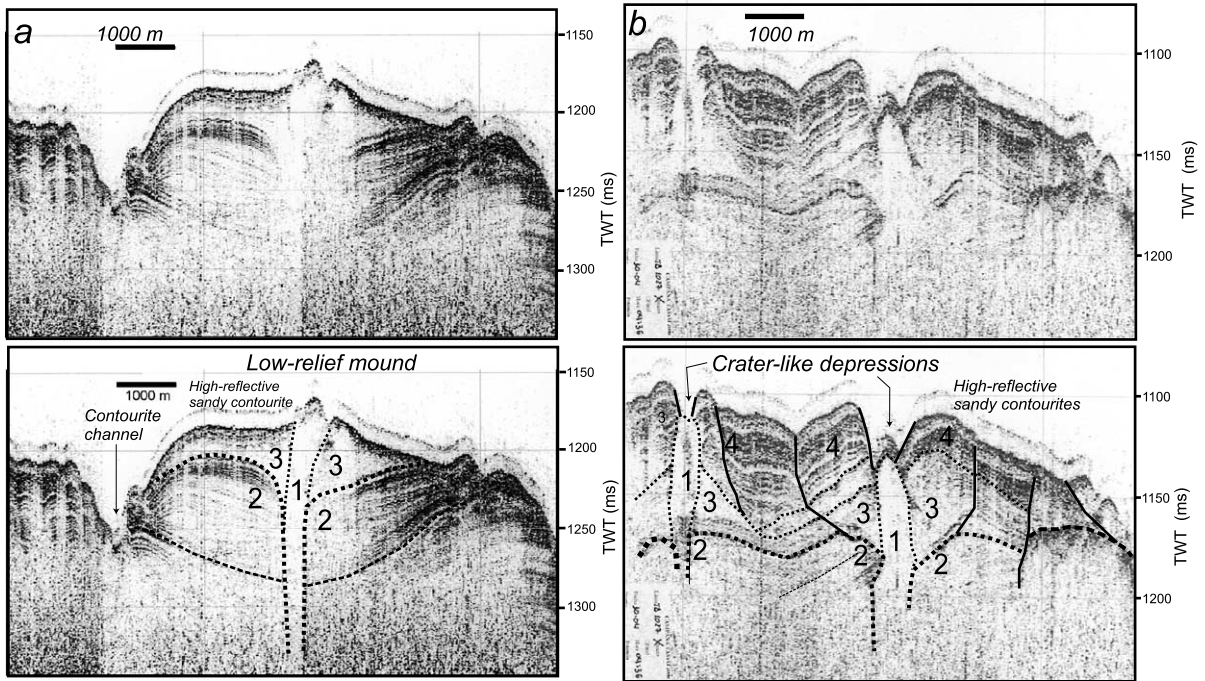


Fig. 11. TOPAS parametric echo-sound profile across small circular depressions observed on the multibeam bathymetry in the TASYO field (see Fig. 4b). (a) Uninterpreted and interpreted seismic profile across a small cone-shaped mound with a very low relief of 10–15 m above sea floor. (b) Uninterpreted and interpreted seismic profile of crater-like depressions: 1 = columnar transparent seismic reflection patterns (feeder channel) that break the: 2 = adjacent well-stratified and dipping host sediment reflectors; 3 = transparent acoustic patterns forming a cone-shaped structure overlapped by: 4 = high-reflective and parallel well stratified reflectors. For location, see Fig. 4b.

columnar, acoustically transparent facies. Normal faults are also identified and arranged in a manner typical for a collapse-type structure. A major discontinuity at 1175 ms TWT, marked by a slightly undulating strong reflector, bends down toward the feeder channel. Two main units are differentiated overlying this discontinuity: a lower unit characterised by low reflectivity, acoustic patterns forming a cone-shaped mound; and an upper unit composed of highly reflective parallel reflectors interfingering with transparent acoustic facies. The sea floor consists of a thin layer of high-reflectivity sediments overlying transparent parallel deposits.

5.5. Mud cones with carbonate chimneys

The term ‘mud cone’ has been applied to asymmetric cone-shaped mounds with steep flanks (up

to 25°) which are characterised by the extensive presence of methane-related pipe-like carbonate chimneys and carbonate slabs but lack mud breccia deposits. The three largest mud cones (Iberico, Cornide and Coruña) identified along the western part of the GDR were dredged and photographed. Dredge samples yielded a large number of pipe-like carbonate chimneys and associated slabs which overlie plastic mud deposits and blue marls (Díaz del Río et al., 2003). Along the ridge that links the Cornide and Coruña mud cones, a line of small mounds, named the Hormigas Ridge, was also found. Dredge hauls from the top of the Hormigas Ridge cones also contained abundant carbonate chimneys and slabs. The main mud mound investigated was the Iberico, a 870 m deep and 165 m tall cone-shaped structure, mainly characterised by an asymmetric profile with steep slopes of 22°–25° and 12°–15° at its

southward and northward flank, respectively (Fig. 12). The southernmost flank was the target of dredges during the Anastasya 2000 cruise. A suite of more than 76 individual structures of chimneys was collected. The chimneys have distinct pipe-like morphologies and vary in length from 0.4 to 1 m (Díaz del Río et al., 2003). Dolomite slabs were also recovered in the region where the chimneys occur. The highly reflective surface observed on Iberico seismic lines is associated with the presence of these carbonate chimneys and slabs (Fig. 12) recovered in this region.

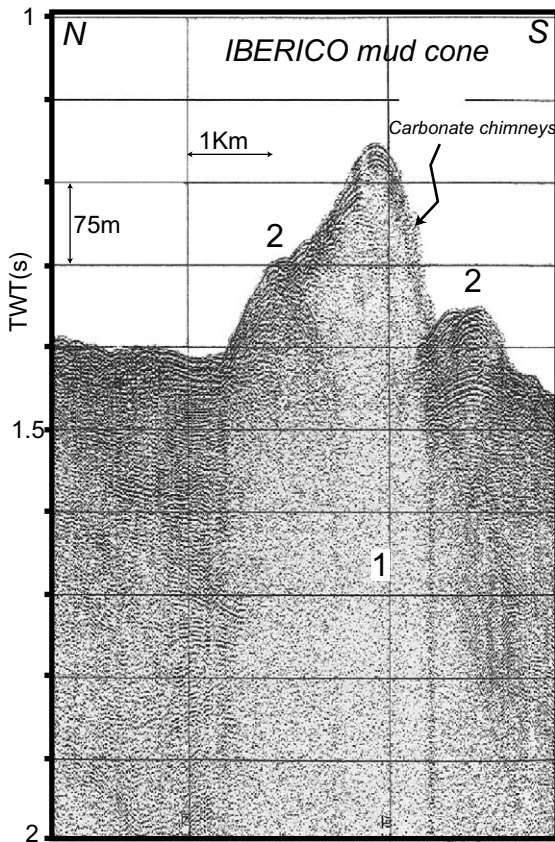


Fig. 12. Single-channel sparker line across the Iberico mud cone. 1=Chaotic and indistinct seismic reflection pattern; 2=high-reflective minor mounds. A suite of more than 76 hydrocarbon-derived carbonate chimneys was collected on the southern side of this structure. For location, see Fig. 3.

6. Discussion

Two of the most dominant morphotectonic features in the Gulf of Cádiz are the GDR and the CDR. Correlation of these NE–SW-trending features with industrial multi-fold seismic and core logs indicates that these longitudinally shaped diapirically controlled ridges are composed mainly of lower–middle Miocene blue marls (Maldonado et al., 1999), associated with tectonic compression of the fronts of the olistostromic/accretionary wedge (Somoza et al., 1999).

6.1. Single, circular mud volcanoes

Single mud volcanoes of the GDR field (Anastasya, Pipoca, Tarsis and Gades) are typical, sub-circular structures rimmed by collapse structures. They range from 0.9 to 2.8 km in diameter and exhibit more than 80–100 m of bathymetric relief. The flanks, which range in slope from 3° to 8°, are formed by several generations of mud flows, which are progressively overlapped by contourite deposits. Gas-saturated mud breccia deposits with a strong H₂S smell compose the flanks of these mud volcanoes. The seismic sequence observed beneath this type of single sub-circular mud volcanoes suggests that it is possible that periods of intense activity of mud breccia ejection alternated with relatively passive periods (Camerlenghi et al., 1995), and is not due to significant differences in physical properties of the host sedimentary sequence. Therefore, we assume that the effects of degassing during initial stages of active mud extrusion may produce sub-circular collapse structures (Figs. 4 and 5) as represented on seismic lines as downward deflections of adjacent deposits (Figs. 6 and 7). These circular depressions become gradually filled by several flows of fluid mud breccia being extruded and expand radially, forming a circular cone-shaped edifice. The slopes of these mud volcano cones, ranging from 3° to 8°, consist mainly of fluidised mud breccia flows which are progressively overlapped by contourites deposited after mud extrusion ceased. This phenomenon is observed in the Pipoca and Tarsis mud volcanoes (Fig. 7) as well as in the Gades mud volcano, at the eastern part of the GDR field at 915 m depth

(Fig. 2), represented by a single circular very low-relief mound, 52 m in height and 0.9 km in diameter. Gravity cores from the crest revealed 3 m of contourite deposits overlying heterometric mud breccia. Other single structures, such as P1 and P2, are observed on multibeam bathymetry (Fig. 3 and Table 1) as very low-relief sea-floor mounds, with large sub-bottom edifices. This points to different stages in the mud volcano activity. Moreover, the prominent mound observed on top of the Anastasya mud volcano, with steep slopes of 13° and thinly covered by contouritic sediments (less than 5 cm), suggests a recent stage of ejection of more viscous muds and probably formation of carbonate crusts (Fig. 6).

6.2. *Complex mud volcano with numerous cones*

A multi-cone mud volcano, named Hespérides, is the largest feature of the TASYO field, with 150 m of bathymetric relief. It has a complex morphology with numerous craters that reach a diameter of more than 3 km. Sampling from the crest of the cones yielded gas-saturated mud breccia deposits mainly composed of clasts of blue marls with strong H₂S smell, carbonate crusts and small calcite chimneys. Sub-sea-floor diapirs and mud volcano cones are formed by leakage through a short feeder channel which is observed in the seismic data. This type of multi-cone mud volcano is similar to that identified in other areas of extensive gas seeps associated with sea-floor-piercing mud diapirs (Ivanov et al., 1996).

6.3. *Oval mud volcanoes associated with slides*

The main characteristic of these oval mud volcanoes is that they are linked by an arcuate ridge resembling a slide scar. Other similar features of mass movement processes are also observed on multibeam bathymetry in the TASYO field. This ridge has a positive relief of more than 275 m between Cibeles and Faro cones, but transforms to a deep depression more than 125 m below the adjacent seabed at the westernmost side of the ridge between Faro and Almazán mud volcanoes. This suggests that this feature was formed by a major slide moving in a S–SW direction, creating

transpressive ridges and fractures by extensional faulting at the head of the slide. Other similar structures are observed at the western side of this ridge feature, but without evidence of associated mud volcanoes.

The major discontinuity that separates underlying offshore dipping seismic units from an upper highly deformed unit (Fig. 10) is interpreted as the detached surface of the slump scar observed on the bathymetric map (Fig. 4b). A series of listric growth faults rooted in this detachment layer are observed, deforming the uppermost sediments. At the same time, widening of feeder channels along this detachment surface and displacement therein suggest a close relationship between the mud volcanism and the formation of the slide (Fig. 10).

The Almazán mud volcano core is interpreted as a sequence of ejected mud breccia deposits alternating with inactive periods during which colonisation by ahermatypic corals, which were probably cemented on carbonate slabs, took place. The uppermost layer of sandy deposits suggests that presently there is no ejection of mud breccia. On the other hand, ‘mousse-like’ muds observed at 70 cm below sea floor (830 m water depth) could be attributed to recent gas hydrate dissociation, although no gas hydrate crystals were recovered from this mud volcano. Further to the south, in similar water depths along the Moroccan margin, gas hydrate crystals were recovered from Ginsburg mud volcano, at a similar core depth in fluidised muds similar to what is observed in the Almazán mud volcano core, so the existence of gas hydrates cannot be ruled out (Mazurenko et al., 2000; Gardner et al., 2001).

6.4. *Low-relief mounds and crater-like depressions*

Ultra-high resolution seismic data of the circular depressions observed on the multibeam bathymetry map (Fig. 4b) revealed the presence of small cone-shaped mounds with very low relief (10–15 m). These small mounds show step-like profiles and benches along their slopes (Fig. 11a). The presence of feeder channels, with cone-shaped transparent reflection patterns and

a positive relief, suggests that this type of structure may be interpreted as small mud volcanoes associated with collapse depressions. Although mud breccia deposits have not been sampled on this type of structure, we suggest that this is probably due to the thickness of contourite deposits in this area with a high sedimentation rate, related to the channels located in this region.

More than 30 circular crater-like depressions (pockmarks) 1–1.2 km in diameter, with steep slopes (20°–25°) and low-relief mounds (10–15 m) and 0.4 km in diameter, characterise the sea-floor morphology of the TASYO field. These depressions are similar to pockmarks as described by Hovland and Judd (1988) and Kelley et al. (1994). Based on these observations, the circular depressions are interpreted as collapse structures related to rising fluids from degassing diapirs. The fluids may be stored in permeable sandy channelled contourite deposits which occur beneath the sea floor (Limonov et al., 1997). Like the mounds discussed earlier, mud breccia deposits are absent on the sea floor. This may be the result of rapid deposition of contourite deposits triggered by the collapse of the feeder channels. In addition, these two types of morphologies may represent different stages in the development of collapse structures; type 1 represents the initial collapse of former mud volcanoes, whereas type 2 represents a later stage of collapse.

6.5. *Mud cones with carbonate chimneys*

The three largest mounds (Iberico, Cornide and Coruña) identified along the western part of the GDR were dredged and photographed. Dredge samples yielded a large number of pipe-like carbonate chimneys and associated slabs which overlie plastic mud deposits and blue marls (Díaz del Río et al., 2003). These mounds are interpreted to be mud cones and not mud volcanoes since mud breccia deposits were not recovered (Camerlenghi et al., 1995).

The chimneys and carbonate slabs are dominated by Fe-enriched dolomite (ankerite) forming aggregates with minor amounts of pyrite, iron oxide, Ta-enriched rutile, zircon and quartz. Abundant, well preserved remains of foraminifera (globiger-

inoids and milioids) composed of Mg calcite are present within the matrix. $\delta^{13}\text{C}$ values indicate that carbonates are moderately depleted in ^{13}C , ranging from –20‰ to –46‰ PDB, interpreted as formed from a mixture of deep thermogenic hydrocarbons and shallow biogenic methane (Díaz del Río et al., 2003). In addition, the abundant pseudo-pyrite framboids are related to the zone of shallow microbial sulphate reduction, a process fundamental to the nourishment of the chemosynthetic cold-seep communities.

7. Conclusions

Extensive mud volcanism, mud diapirism and carbonate chimneys related to hydrocarbon-rich fluid venting are observed throughout the Spanish–Portuguese margin of the Gulf of Cádiz. All the mud volcanoes and diapirs addressed in this paper lie in the region of olistostrome/accretionary complex units which were emplaced in the Late Miocene in response to NW-directed convergence between the African and Eurasian plates. The interpretation of multibeam bathymetry, high resolution seismic reflection profiling and core data leads to the following conclusions:

(1) The orientation of the morphological elements corresponds to the two large morphotectonic features: the Guadalquivir and Cádiz Diapiric Ridges (GDR and CDR), which are longitudinally shaped diapirs that trend NE–SW and consist of lower–middle Miocene plastic marly clays of the olistostromic M1 unit (Maldonado et al., 1999).

(2) Sub-circular features identified on multibeam bathymetry may be defined as mud volcanoes, mud cones and crater-like collapse structures, depending on their morphology, seismic expression and sedimentary nature (mud breccias).

The origin of all these hydrocarbon-related fluid venting structures are associated with recent compressional tectonics of the shale/salt deposits of the olistostrome/accretionary complex units, which were emplaced in the Late Miocene, in response to the NW-directed convergence between the African and Eurasian plates (Maldonado et

al., 1999). The GDR and CDR longitudinally shaped diapirs are interpreted as caused by lateral compressional stresses that are pressing up and squeezing plastic marly clay deposits (lower–middle Miocene M1 unit) of the front of the olistostrome/accretionary complex. Mud cones with extensive pipe-like chimneys located at the westernmost side of the GDR are related with high-angle thrust faults. The location of single circular mud volcanoes at the northern front of this ridge suggests that they are associated with overpressure compartments developed beneath thrusting structures, which provide avenues to the sea floor for hydrocarbon-enriched fluids (Lowrie et al., 1999). Large mud volcanoes of the TASYO field are linked with isolated sea-floor-piercing diapirs developed between the CDR and GDR.

We suggest that some of the widespread shallow fluid venting on the sea floor in the TASYO field may be related to the destabilisation of gas hydrate-rich sediments in contact with Mediterranean Outflow Water (Somoza, 2001). This mechanism may be responsible for the complex sea-floor morphology observed on multibeam bathymetry in the TASYO field, which is characterised by numerous crater-like collapse structures and slides, which is similar to processes inferred for the Blake Ridge (Dillon et al., 2001).

Acknowledgements

This paper is dedicated to the memory of Jesus Baraza, our colleague. This research was funded by the Spanish Marine Science and Technology Program, under the TASYO Project No. 98-0209, and in the framework of the Spanish–Portuguese agreement for scientific cooperation. Contributions by J.M. Gardner to this project were supported by the Office of Naval Research PE#0601153N. The authors thank all those who participated in the research cruises of the TASYO project, especially the captains and crews of both the R/V *Cornide de Saavedra* and the R/V *Hespérides*. J.M. Serna helped with the GIS-building and figures. We are grateful to F. Sanchez for electronic support during seismic acquisition and

to P. Rodriguez for his helpful support during the acquisition of the multibeam data. Also thanks to captain, technicians and crew of the R/V *Professor Logachev* for their kind assistance during the TTR10 IOC–UNESCO cruise. The advice and criticism from the reviewers, A. Camerlenghi and P. Vogt is sincerely appreciated. Also, we thank John Woodside and Alexei Suzyumov for their valuable input.

References

- Baraza, J., Ercilla, G., 1996. Gas-charged sediments and large pockmark like features on the Gulf of Cadiz slope (SW Spain). *Mar. Petrol. Geol.* 13, 253–261.
- Battista, B.M., Lowrie, A., Makarov, V., Moffett, S.J., Somoza, L., 2000. Lateral tectonics in the Gulf of Mexico, Gulf of Cadiz, and the Middle America Trench: Impacts on hydrocarbon accumulations. *Am. Assoc. Petr. Geol. Annual Convention*, New Orleans, LA, USA, paper 3059.
- Berástegui, X., Banks, C.J., Puig, C., Taberner, C., Waltham, D., Fernández, M., 1998. Lateral diapiric emplacement of Triassic evaporites at the southern margin of the Guadalquivir Basin, Spain. In: Mascle, A., Puigdefábregas, C., Luterbacher, H., Fernandez, M. (Eds.), *Cenozoic Foreland Basins of Western Europe*. *Geol. Soc. Spec. Publ.* 134, pp. 49–68.
- Blankenship, C.L., 1992. Structure and paleogeography of the External Betic Cordillera, southern Spain. *Mar. Petrol. Geol.* 9, 256–264.
- Brown, K., Westbrook, G.K., 1988. Mud diapirism and subcretion in the Barbados Ridge accretionary complex: the role of fluids in accretionary processes. *Tectonics* 7, 613–640.
- Camerlenghi, A., Cita, M.B., Della Vedova, B., Fusi, N., Mirabile, L., Pellis, G., 1995. Geophysical evidence of mud Diapirism on the Mediterranean Ridge accretionary complex. *J. Mar. Geophys. Res.* 17, 115–141.
- Díaz del Río, V., Somoza, L., Martínez-Frías, J., Hernández-Molina, F.J., Lunar, R., Fernández-Puga, M.C., Maestro, A., Terrinha, P., Llave, E., García, A., García, A. C., Vázquez, J.T., 2001. Carbonate chimneys in the Gulf of Cadiz: Initial report of their petrography and geochemistry. *Proc. Int. Conf. Geological Processes on Deep-Water European Margins. IOC/UNESCO Workshop Report 175*, pp. 53–54.
- Díaz del Río, V., Somoza, L., Martínez-Frías, J., Mata, M.P., Delgado, A., Hernández-Molina, F.J., Lunar, R., Martín-Rubí, J.A., Maestro, A., Fernández-Puga, M.C., León, R., Llave, E., Medialdea, T., Vázquez, J.T., 2003. Vast fields of hydrocarbon-derived carbonate chimneys related to the accretionary wedge/olistostrome of the Gulf of Cádiz. *Mar. Geol.*, S0025-3227(02)00687-4.
- Dillon, W.P., Nealon, J.W., Taylor, M.H., 2001. Seafloor collapse and methane venting associated with gas hydrate on the Blake Ridge - Causes and implications to seafloor stability and methane release. In: Paull, C.K., Dillon, W.K.

- (Eds.), *Natural Gas Hydrates: Occurrence, Distribution and Detection*. AGU Geophys. Monogr. 124, pp. 211–233.
- Fernández-Puga, M.C., Somoza, L., Lowrie, A., Maestro, A., León, R., Díaz del Río, V., 2000. Fluid seeps associated with gravity spreading of salt/shale along the Gulf of Cádiz continental slope. *Proc. Int. Conf. Geological Processes on European Continental Margins*. IOC/UNESCO Workshop Report 168, pp. 21–22.
- Flynch, J.A., Bally, A.W., Wu, S., 1996. Emplacement of a passive margin evaporitic allochthon in the Betic Cordillera of Spain. *Geology* 24, 67–70.
- Gardner, J.M., 1999. Mud volcanoes on the Moroccan Margin. *EOS Trans. AGU* 80, 483.
- Gardner, J.M., 2001. Mud volcanoes revealed and sampled on the western Moroccan continental margin. *Geophys. Res. Lett.* 28, 334–342.
- Gardner, J.M., Vogt, P.R., Somoza, L., 2001. The possible effect of the Mediterranean Outflow Water (MOW) on gas hydrate dissociation in the Gulf of Cádiz. *EOS Trans. AGU* 82 (47), Fall. Meet. Suppl. Abstracts OS12B-0418.
- Guliyev, I.S., Feizullayev, A.A., 1997. All about mud volcanoes. *Geology Institute Azerbaijan Academy of Sciences, Nafta-Press, Baku, Azerbaijan*, 52 pp.
- Hedberg, H.D., 1974. Relation of methane generation to undercompacted shales, shale diapirs and mud volcanoes. *Am. Assoc. Petr. Geol. Bull.* 58, 661–673.
- Hovland, M., Judd, A., 1988. Seabed Pockmarks and Seepages: Impact on Geology, Biology and the Marine Environment. *Graham and Trotman, London*, 293 pp.
- Ivanov, M.K., Limonov, A.F., van Weering, Tj.C.E., 1996. Comparative characteristics of the Black Sea and Mediterranean Ridge mud volcanoes. *Mar. Geol.* 132, 253–271.
- Ivanov, M.K., Kenyon, N., Nielsen, T., Wheeler, A., Monteiro, J., Gardner, J., Comas, M., Akhmanov, G., Akhmetzhanov, A., Scientific Party of the TTR-9 cruise, 2000. Goals and principal results of the TTR-9 cruise. *Proc. Int. Conf. Geological Processes on European Continental Margins*. IOC/UNESCO Workshop Report 168, pp. 3–4.
- Ivanov, M.K., Pinheiro, L., Stadnitskaia, A., Blinova, V., 2001. Hydrocarbon seeps on Deep Portuguese Margin. *Final Proc. 11th Meeting of the European Union of Geosciences, Strasbourg, France, CC11*, p. 160.
- Kelley, J.T., Dickson, S.M., Belknap, D.F., Bernhardt, W.A., Henderson, M., 1994. Giant seabed pockmarks: evidence for gas escape from Belfast Bay, Maine. *Geology* 22, 59–62.
- León, R., Somoza, L., Ivanov, M.K., Diaz-del-Río, V., Lobato, A., Hernandez-Molina, F.J., Fernandez-Puga, M.C., Maestro, A., Medialdea, T., Alveirinho, J., Vazquez, J.T., 2001. Seabed morphology and gas venting in the Gulf of Cadiz mudvolcano area: Imagery of multibeam data and ultra-high resolution data. *Proc. Int. Conf. Geological Processes on deep-water European margins*. IOC/UNESCO Workshop Report 175, pp. 43–45.
- Limonov, A.F., Van Weering, Tj.C.E., Kenyon, N.H., Ivanov, M.K., Meisner, L.B., 1997. Seabed morphology and gas venting in the Black Sea mudvolcano area: observations with the MAK-1 deep-tow sidescan sonar and bottom profiler. *Mar. Geol.* 137, 121–136.
- Lowrie, A., Hamiter, R., Moffett, S., Somoza, L., Maestro, A., Lerche, I., 1999. Potential pressure compartments sub-salt in the Gulf of Mexico and beneath massive debris flows in the Gulf of Cadiz. 19th Annual Bob. F. Perkins Conference Abstracts, *Advanced Reservoir Characterization for the 21st Century*. GCSSEPM Foundation, Houston, TX, pp. 271–280.
- Lowrie, A., Somoza, L., Battista, B.M., Moffett, S.J., Lerche, I., 2000. Hydrocarbon potential of the Gulf of Cadiz increases with greater thermal maturity. *Am. Assoc. Petr. Geol. Annual Meeting, New Orleans, LA, USA*, paper 3343.
- Maldonado, A., Somoza, L., Pallarés, L., 1999. The Betic orogen and the Iberian-African boundary in the Gulf of Cadiz: geological evolution (Central North Atlantic). *Mar. Geol.* 155, 9–43.
- Mazurenko, L.L., Soloviev, V.A., Gardner, J.M., 2000. Hydrochemical features of gas hydrate-bearing mud volcanoes, offshore Morocco. *Proc. Int. Conf. Geological processes on European continental margins*. IOC/UNESCO Workshop Report 168, pp. 18–19.
- Milkov, A.V., 2000. Worldwide distribution of submarine mud volcanoes and associated gas hydrates. *Mar. Geol.* 167, 29–42.
- Nelson, C.H., Maldonado, A., 1999. The Cadiz margin study off Spain: An introduction. *Mar. Geol.* 155, 3–8.
- Orange, D.L., Greene, H.G., Reed, D., Martin, J.B., McHugh, C.H., Ryan, W.B.F., Maher, N., Stakes, D., Barry, J., 1999. Widespread fluid expulsion on a translational continental margin: Mud volcanoes, fault zones, headless canyons, and organic-rich substrate in Monterey Bay, California. *GSA Bull.* 111, 992–1009.
- Perconig, E., 1960–62. Sur la constitution géologique de l'Andalousie Occidentale, en particulaire du bassin du Guadalquivir (Espagne Méridionale). In: *Livre Mémoire du Professeur Paul Fallot. Mémoires hors-Série de la Société géologique de France*, pp. 229–256.
- Roberts, H.H., Carney, R.S., 1997. Evidence of episodic fluid, gas, and sediment venting on the northern Gulf of Mexico Continental Slope. *Econ. Geol.* 92, 863–879.
- Somoza, L., 2001. Hydrocarbon seeps, gas hydrates, and carbonate chimneys in the Gulf of Cadiz: an example of the interaction between tectonic and oceanographic controlling factors. *Proc. Int. Conf. Natural Hydrocarbon Seeps, Global Tectonics and Greenhouse Gas Emissions, ESF-LESF Workshop, Delft, The Netherlands*, pp. 18–19.
- Somoza, L., Díaz del Río, V., Hernández-Molina, F.J., León, R., Lobato, A., Alveirinho, J.M., Rodero, J., TASYO team, 2000. New discovery of a mud-volcano field related to gas venting in the Gulf of Cadiz: Imagery of multibeam data and ultra-high resolution data. *Final Proc. 3rd Int. Symp. Iberian Atlantic Continental Margin, Faro, Portugal*, pp. 397–398.
- Somoza, L., Ivanov, M.K., Pinheiro, L., Maestro, A., Lowrie, A., Vazquez, J.T., Gardner, J.M., Medialdea, T., Fernandez-Puga, M.C., 2001. Structural and tectonic control of

- fluid seeps and mud volcanoes in the Gulf of Cadiz. Int. Conf. Geological Processes on Deep-Water European Margins. IOC/UNESCO Workshop Report 175, pp. 41–42.
- Somoza, L., Maestro, A., Lowrie, A., 1999. Allochthonous Blocks as Hydrocarbon Traps in the Gulf of Cadiz. Offshore Technology Conf. Proc., OTC-12202, pp. 571–577.
- Stadniskaia, A., Ivanov, M., Gardner, J., 2000. Hydrocarbon gas distribution in mud volcanic deposits of the Gulf of Cadiz. Preliminary results. Int. Conf. Geological Processes on European Continental Margins. IOC/UNESCO Workshop Report 168, pp. 17–18.
- Torelli, L., Sartori, R., Zitellini, N., 1997. The giant chaotic body in the Atlantic ocean off Gibraltar. New result from a deep seismic reflection survey. *Mar. Petrol. Geol.* 14, 125–138.
- Vázquez, J.T., Somoza, L., Medialdea, T., Maestro, A., Maldonado, A., Vegas, R., 2001. Olistostrome tectonic fronts under the Eurasia-Africa Convergence in the Gulf of Cadiz. Final Proc. Int. Workshop on the Western Part of Eurasia-Africa Plate Boundary (Azores-Tunisia), San Fernando, Cádiz, Spain. *Boletín ROA* 3, 132–133.